RICE UNIVERSITY

Inter-beam Interference Management with Side-channels

by

Andrew Zhou Kwong

A THESIS SUBMITTED
IN PARTIAL FULFILLMENT OF THE
REQUIREMENTS FOR THE DEGREE

Master of Science

APPROVED, THESIS COMMITTEE:

Dr. Ashutosh Sabharwal, *Chair*
Professor of Electrical and Computer Engineering

Dr. Behnaam Aazhang
J.S. Abercombie Professor of Electrical and Computer Engineering

Dr. Edward Knightly
Professor of Electrical and Computer Engineering

HOUSTON, TEXAS
DECEMBER 2016

Abstract

Inter-beam Interference Management with Side-channels

by

Andrew Zhou Kwong

Inter-beam interference is a problem that afflicts conjugate beamforming systems, which are being considered for massive MIMO downlink systems. To deal with inter-beam interference, we propose allowing users to act as mutual relays over orthogonal side-channels to enable V-BLAST for single-antenna users in a system called cooperative inter-beam nulling and cancellation (CINC). In addition to CINC, we also propose systems with only individual components of V-BLAST are enabled over side-channels. For the decorrelator portion of V-BLAST, we propose cooperative inter-beam nulling (CIN), and for the successive interference cancellation portion of V-BLAST, we propose cooperative inter-beam cancellation (CIC).

The key difference between V-BLAST in a multiple antenna receiver and V-BLAST in single antenna users over side-channels is that side-channel resources are limited in power budget and spectrum usage. Therefore, we study how the proposed strategies perform when the number of mutual relayers is limited by side-channel SNR and available side-channel time-bandwidth. We compute the user's effective SINR for each method in Rayleigh channels, then perform numerical simulations to find the achievable rate given side-channel resources.

From our results, we characterize the improvement by showing the percentage increase in sum-rate that can be achieved by each method for different amounts of time-bandwidth resources. In our simulation scenario with Rayleigh channels, 100 base station antennas, and 8 users, we show that CINC, the full V-BLAST over side-channel system, can achieve 21 % average sum-rate improvement with time-bandwidth limited to 3 times the amount available on the main channel, and 139 % with 12 times the time-bandwidth, where there is full cooperation.

We then use our numerical simulations to outline different regimes of side-channel resources where the amplify-and-forward relayers of CINC should be prioritized and where the decode-and-forward relayers of CINC should be prioritized. We find that the amplify-and-forward relaying should be prioritized in general, except when side-channel SNR is less than 5 dB and when side-channel SNR is greater than 20 dB, but time-bandwidth resources on the side-channel are less than the number of users times the amount available on the main channel, where decode-and-forward relaying should be prioritized.

Acknowledgements

I would like to thank my advisor Dr. Ashutosh Sabharwal for his support and guidance. The lessons he has taught me over the course of this thesis are lessons that I will carry with me beyond graduate school.

I would also like to thank the members of my committee, Dr. Behnaam Aazhang and Dr. Edward Knightly, for their time and effort in reviewing my work.

The peers, friends, and mentors I've met at Rice have been invaluable for giving me advice and keeping me motivated, with a special mention towards Dr. Evan Everett for his guidance.

Finally, I'd like to thank my parents for supporting me in this graduate school endeavor.

Contents

List of Figures

Chapter 1

Introduction

Massive MIMO is an emerging technology in which antenna arrays scale up the number of antennas by orders of magnitudes. Scaling up the number of antennas can improve the energy efficiency and, more importantly, enable MIMO systems to serve many more terminals simultaneously. Massive MIMO can therefore improve spectral efficiency on the order of 10 times or more, which is increasingly important in an increasingly spectrum limited environment [?].

Conjugate beamforming is an efficient method of realizing multi-user massive MIMO downlink. Previous works have shown that conjugate beamforming is capable of reducing the overhead necessary for a MIMO beamforming systems, especially massive MIMO systems [1] while still maintaining optimal performance when the number of base station antennas approaches infinity [2] [3].

However, inter-beam interference, also known as inter-user interference, inhibits the performance of conjugate beamforming in the finite antenna regime. Inter-beam interference is the interference caused by a beam directed towards one user leaking into the transmission towards another user, causing the signals to interfere with one another. The problem of inter-beam interference becomes especially prominent as the number of users served simultaneously increases.

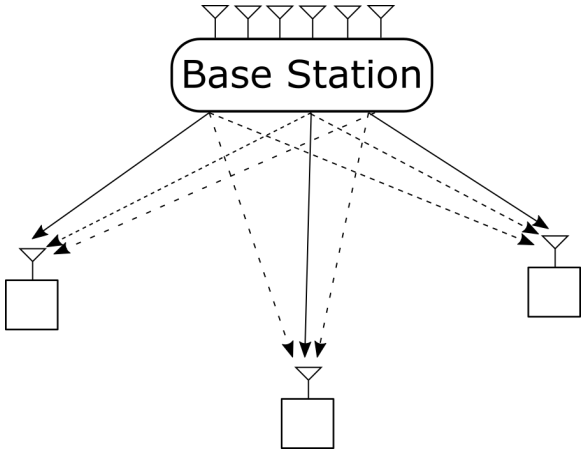

Figure 1.1: CINC User Processing

Given a downlink conjugate beamforming system, we examine methods of managing inter-beam interference by leveraging receiver-side resources. In particular, we focus on V-BLAST as a receiver-side interference management technique. V-BLAST is a multiplexing technique that achieves capacity in fast-fading channels with a simple architecture, and it is often even considered synonymous with spatial multiplexing [4]. The variation of V-BLAST we consider is comprised of a decorrelator bank combined with successive interference cancellation.

V-BLAST is typically not considered for downlink systems, however, because it requires that receivers have a greater number of antennas than interferers [5] and that different data streams share their decoded symbols. In downlink systems, users typically only have a single antenna for the specified band and no wired connection for different streams to share decoded information.

Therefore, to enable V-BLAST for a group of users with only a single antenna on the main channel, we propose using side-channels to allow each user to overcome the lack of antennas. Side-channels are device-to-device channels in orthogonal frequency bands through which users can share information [6]. Utilizing side-channels leverages an existing trend where mobile devices can simultaneously access increasing numbers

of frequency bands, such as accessing both the cellular band and the ISM band. Side-channels can be used for relaying to emulate how information is shared in a single multiple-antenna receiver through wired connections, thus giving the users the information needed to perform V-BLAST.

V-BLAST requires two types of information shared for each data stream. First, the raw analog signal from different antennas needs to be shared in order to enable the decorrelator. Over side-channels, the equivalent counterpart to sharing the analog signal over a wired connection is *amplify-and-forward relaying*. Second, the decoded symbols must be shared in order to perform successive interference cancellation (SIC). Over side-channels, the equivalent counterpart to sharing the decoded symbols is *decode-and-forward relaying*. Using each type of relaying can therefore enable V-BLAST over side-channels.

In addition to examining the full V-BLAST system over side-channels, we also propose and examine systems that have each component individually, that is, a decorrelator only system and a SIC only system. Doing so allows us to understand the impact of each individual component, as well as provide simpler alternatives to the full V-BLAST over side-channels system.

Previous work on relaying for interference management has focused on cases with specific numbers of users or relayers. For example, on the information theoretic side, works such as [7] and [8] derive bounds on the specific case of systems with two source-destination pairs and a single relayer. The most similar previous work to our current work [9] requires every user in the system to act as a mutual relay in order to implement a decorrelator for a zero-forcing beamforming system.

Unlike previous works, we do not specify a particular number of relayers, and instead examine what happens when the number of mutual relayers is constrained by side-channel resources. The side-channel spectrum is often shared between different

applications, and using the side-channel consumes a certain amount of power. Therefore, only a limited number of users can participate in the relaying, depending on the availability of the side-channel resources. The resource constraints described in our work are represented by the SNR of side-channel transmissions as well as time-bandwidth resources on the side-channel. Constraints on the SNR represent a restriction on the power available for each user, and constraints on the time-bandwidth resources represent the availability of spectral resources.

In addition to proposing our strategies, we have two main goals in our work. The first is to find how much improvement can be expected from our proposed strategies depending on the amount of available side-channel resources. The second is to develop heuristics on how to allocate side-channel resources to each component of V-BLAST when side-channel resources are limited, that is, how many amplify-and-forward relayers and how many decode-and-forward relayers should be supported for a given amount of side-channel resources.

Our contributions in this work accomplish these goals in three steps. First, we detail the three strategies proposed in this paper. The first strategy, cooperative inter-beam nulling (CIN), comprises the decorrelator component of V-BLAST. The second strategy, cooperative inter-beam cancellation (CIC), comprises the SIC component of V-BLAST. Examining systems with each individual component helps with our second goal of developing heuristics for determining how to allocate side-channel resources to each component and provides an intermediate step towards understanding the full system. The third strategy, cooperative inter-beam nulling and cancellation (CINC), comprises the full V-BLAST over side-channel system.

Second, we analytically show the average SINR for Rayleigh channels with a given number of cooperators for each strategy. By analytically showing the average SINR, we can contribute to our first goal of finding how much improvement can be ex-

pected by showing how much the signal-to-interference ratio (SIR) improves when our strategies are implemented. We find that a user's SIR improves superlinearly with the number of unique, contributing relayers. We also show the trade-off in how noise is amplified when using the decorrelator, therefore finding that the decorrelator is only effective in an interference-dominated rather than a noise-dominated system.

Third, we numerically simulate the achievable sum-rate of the three methods under constraints on the available power or time-bandwidth on the side-channel for several different cellular scenarios. We accomplish our first goal by showing that the achievable rate is significantly improved with each strategy. We then accomplish our second goal by showing that there exist different side-channel resource regimes at which either amplify-and-forward or decode-and-forward relayers are more effective.

Chapter 2

System Model

We consider a single cell with an M-antenna base station and K single-antenna downlink users. For our analysis, we assume that the base station has perfect, genie-aided channel state information at the transmitter (CSIT) and that the users have perfect, genie-aided channel state information at the receiver (CSIR). The main channel and the side-channels are distributed as a Rayleigh fading channel. On the main channel, in each block, the base station transmits to the users with *conjugate beamforming* such that each user receives

$$y_j = c_{cj}\mathbf{h}_j\mathbf{H}^H\mathbf{s} + n_j, \tag{2.1}$$

where y_k is the received symbol at User k, c_{cj} is a constant that adjusts the total transmit power, $\mathbf{h}_k$ is the k-th row of the channel fading matrix $\mathbf{H}$, $\mathbf{H}^H$ is the precoding matrix given by the conjugate transpose of the channel fading matrix $\mathbf{H}$, $\mathbf{s}$ is the symbol vector containing the symbols s_k for each user, and n_k is the additive Gaussian noise term with variance N_0. We assume that the symbols sent to each user are uncorrelated, that is,

$$\mathbb{E}[\mathbf{s}\mathbf{s}^H] = I_K,$$

where I_K is a $K \times K$ identity matrix.

The constant c_{cj} is chosen such that the average total power transmitted is equal to P_M, that is, $\mathbb{E}[\mathbf{x}^T\mathbf{x}] = P_M$, where $\mathbf{x}$ is the transmit vector, giving the following expression:

$$c_{cj} = \sqrt{\frac{P_M}{\mathbb{E}[\mathsf{Tr}(\mathbf{H}\mathbf{H}^H)]}}, \tag{2.2}$$

where Tr is the trace operation.

On the side-channel, users transmit orthogonally in either time or frequency. Each user is capable of broadcasting such that other users receive

$$y_{jk} = \hat{h}_{jk}x_j + n_{jk}, \tag{2.3}$$

where y_{jk} is the symbol received by user k from user j, $\hat{h}_{jk}$ is the fading channel between user j and user k, x_j is the broadcast symbol from user j, and n_{jk} is the noise term with power $N_{0,s}$. The power of the broadcast symbols x_j are chosen such that the average received power for each user is given by $E[|\hat{h}_{jk}x_j|^2] = P_S$.

Chapter 3

Cooperative Strategies

In general, the cooperative interference management strategies described here involve a subset of users broadcasting information that other users can use to reduce the number of effective interferers. The type of information that is broadcasted depends on the type of cooperation being performed.

In our cooperation framework, the total set of users U has subsets of users called cooperation groups, denoted as $C_i \subset U$, that are capable of cooperating with one another. There is no overlap between cooperating groups, that is, $C_i \cap C_k = \emptyset \quad \forall \quad i \neq k$. We assume that users form cooperation groups in local clusters that are out of range from each other, such that users in different cooperation groups receive no side-channel broadcasts from other cooperation groups. We denote the number of cooperating groups as κ, and the union of the cooperating groups makes up the full set of users, that is, $\cup_{i=1}^{\kappa} C_i = U$.

Within each cooperation group C_i, there is a relaying group $B_i \in C_i$ comprised of all the users that broadcast on the side-channel. Users in the relaying group either perform amplify-and-forward relaying, which we denote as A_i, or decode-and-forward relaying, which we denote as D_i, or both, such that $B_i = A_i \cup D_i$. Each type of relaying will be described in further detail in each strategy's subsection. Additionally,

we denote the non-relaying users within each cooperation group as V_i such that $V_i \cup B_i = C_i$. For the purposes of the analysis in this section, we assume that the system has already assigned users to their corresponding groups.

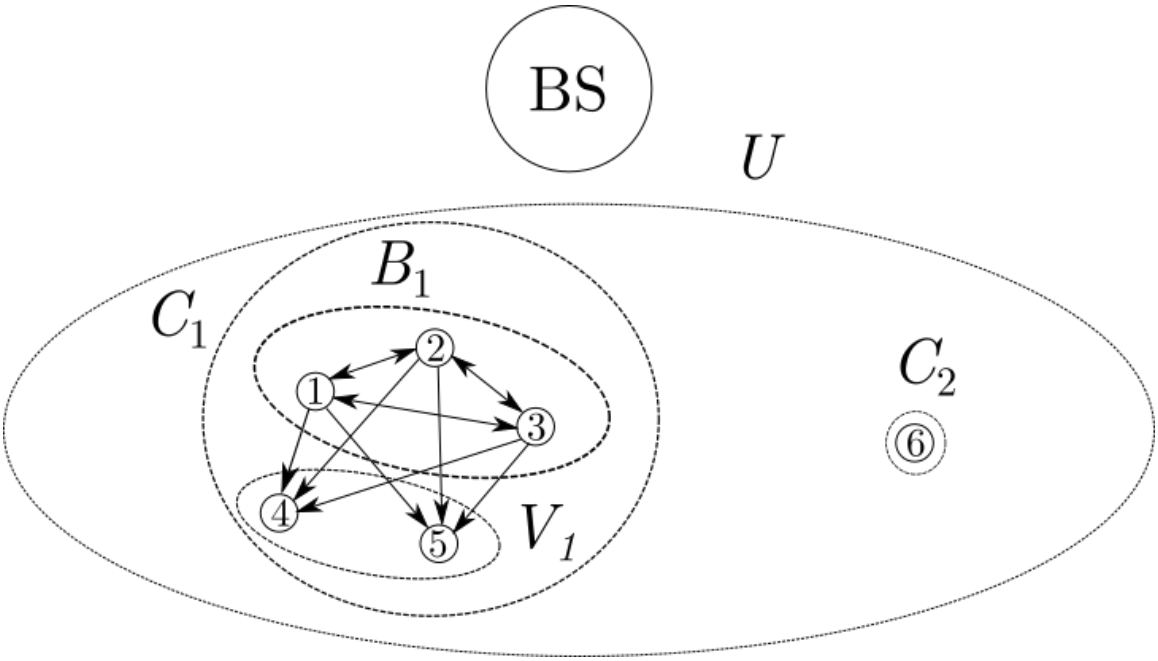

Figure 3.1: Illustration of set notation

Each cooperative strategy is comprised of variations on the same three steps. The first step is conjugate beamforming on the main channel. The second step is the relaying step, in which users share information by broadcast relaying on the side-channel. The type of relaying depends on the strategy. The third step is the processing step, in which the information shared over the side-channel is utilized to reduce interference.

In the following sections, we will describe in detail the relaying steps and processing steps performed in each cooperative strategy. We will then give an expression for the symbol estimate obtained after the processing step.

3.1 Cooperative Inter-beam Nulling

Cooperative Inter-beam Nulling (CIN) is the amplify-and-forward based downlink interference management strategy that was briefly presented in [10] and will be presented in more detail in this paper. As a summary of CIN, users amplify and broadcast the signal received on the main channel to the other users in the cooperation group on the side-channel. The users that receive the broadcasted signals can then form nulls towards the interferers from the broadcasters using a decorrelator. A figure of the process taken by users is provided in Fig. 3.2.

As stated before, we divide the strategy into three steps. The first step, conjugate beamforming on the main channel, has already been explained in the system model. The details on the relaying step and the processing step are described in the subsequent subsections.

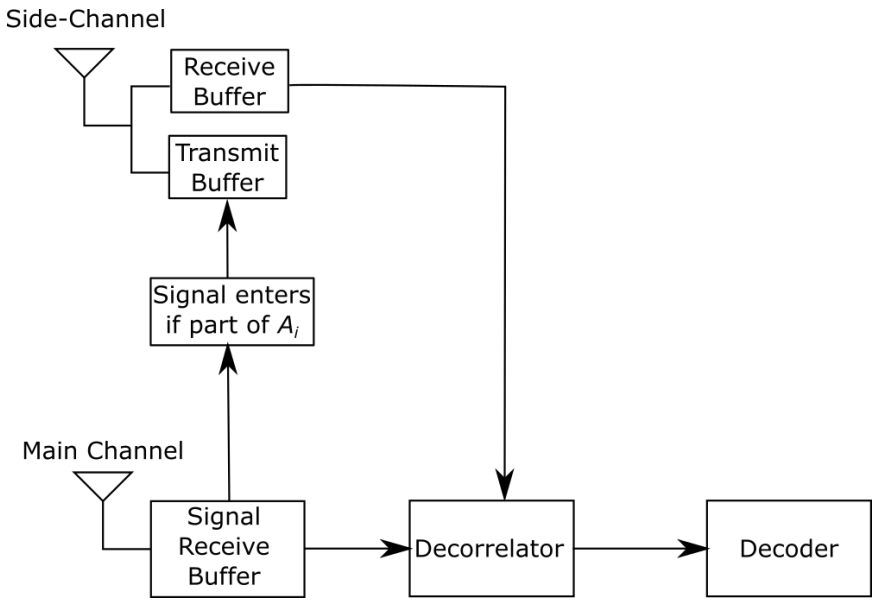

Figure 3.2: CIN User Architecture

3.1.1 Relaying Step

In CIN, the relaying step involves using amplify-and-forward relaying to share the analog signal obtained to other users. Any amplify-and-forward relaying user, which we denote as any User j with $j \in A_i$, broadcasts on the side-channel such that any other user, which we denote as User k with $k \in C_i, j \neq k$, receives

$$y_{jk} = a_j \hat{h}_{jk} y_j + n_{jk} \tag{3.1}$$

$$= a_j \hat{h}_{jk} (c_{cj} \mathbf{h}_j \mathbf{H}^H \mathbf{s} + n_j) + n_{jk}, \tag{3.2}$$

where a_j is the amplification factor determined by the power budget.

The receiving User k can normalize the relaying signals such that

$$y'_{jk} = c_{cj} \mathbf{h}_j \mathbf{H}^H \mathbf{s} + n_j + \frac{n_{jk}}{a_j \hat{h}_{jk}}.$$

3.1.2 Processing Step

Each user puts the received signals, both from the amplify-and-forward relayers and the main-channel, together in a signal vector. The signal vector will have the form

$$\mathbf{Y}_k = c_{cj} \mathbf{H}_k \mathbf{H}^H \mathbf{s} + \mathbf{n}_k, \tag{3.3}$$

where $\mathbf{Y}_k$ is the column vector containing the main-channel signal y_k and normalized relayed signals y'_{jk} for $j \in A_i, j \neq k$, $\mathbf{H}_k$ is the matrix comprised of the rows $\mathbf{h}_l$ with $l \in A_i \cup \{k\}$, and $\mathbf{n}_k$ is a column vector containing n_k and $n_j + n_{jk}/(a_j \hat{h}_{jk})$ for $j \in A_i, j \neq k$. Note that when $k \in A_i$, that is, when User k performs amplify-and-forward relaying, $\mathbf{Y}_k$, $\mathbf{H}_k$, and $\mathbf{n}_k$ each have $|A_i|$ rows, while when $k \in V_i$, that is, when User k does not relay its signal, $\mathbf{Y}_k$, $\mathbf{H}_k$, and $\mathbf{n}_k$ each have $|A_i| + 1$ rows. The

notation $|A_i|$ refers to the cardinality of the set, which in this case means the number of users that perform amplify-and-forward relaying.

With the signal vector $\mathbf{Y}_k$, User k can then obtain the symbol estimate by applying the decorrelator as described in [11], giving

$$F_k = \mathbf{r}_k(\mathbf{H}_k\mathbf{H}_k^H)^{-1}, \tag{3.4}$$

where $\mathbf{r}_k$ is an indicator row vector with components $\mathbf{r}_k, i = 1$ when index i corresponds to User k and $\mathbf{r}_k, i = 0$ otherwise.

Applying the decorrelator yields the symbol estimate

$$\begin{aligned}\hat{\mathbf{s}}_k &= F_k\mathbf{Y_k} \\ &= \mathbf{r}_k(\mathbf{H}_k\mathbf{H}_k^H)^{-1}(\mathbf{H}_k\mathbf{H}^H\mathbf{s} + \mathbf{n}_k) \\ &= \underbrace{c_{cj}s_k}_{\text{signal}} + \underbrace{c_{cj}\mathbf{r}_k\mathbf{H}_k^{H+}\mathbf{H}_{k,F}^H\mathbf{s}_{k,F}}_{\text{interference}} + \underbrace{\mathbf{r}_k(\mathbf{H}_k\mathbf{H}_k^H)^{-1}\mathbf{n}_k}_{\text{noise}},\end{aligned} \tag{3.5}$$

where $\mathbf{H}_{k,F}$ is a matrix comprised of the rows $\mathbf{h}_l$ with $l \notin A_i \cup \{k\}$, and $\mathbf{s}_k^c$ is comprised of the symbols s_l with $l \notin A_i \cup \{k\}$.

3.2 Cooperative Inter-beam Cancellation

Cooperative Inter-beam Cancellation (CIC) is the interference management strategy that uses decode-and-forward relaying for successive interference cancellation. CIC operates as a distributed successive interference cancellation in that the decoded signal from one user can be used to subsequently cancel the interference of subsequent users. As a summary of CIC, users decode their own signals and broadcast them to the other users in the cooperation group over the side-channel. Subsequent users can then subtract out interference terms by using the decoded signals from other users.

The process is described in Fig. 3.3, and details on the relaying and processing steps are described below.

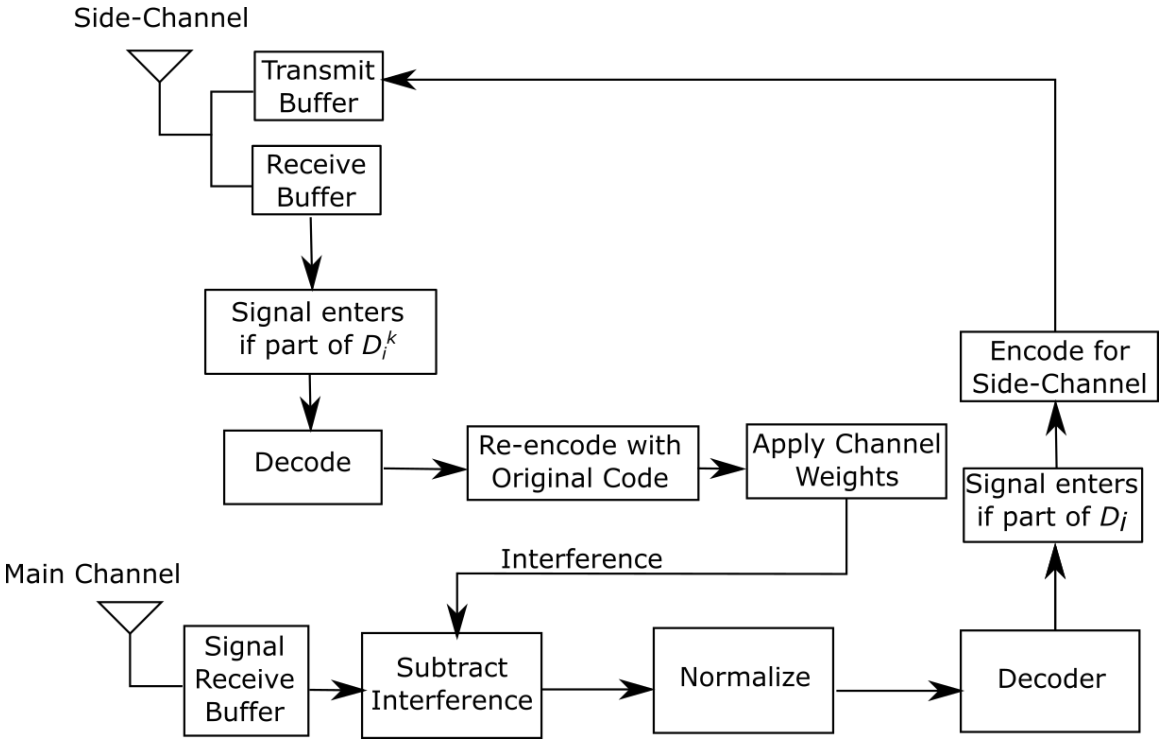

Figure 3.3: CIC User Architecture

3.2.1 Relaying Step

A broadcasting decode-and-forward user, which we denote as User j with $j \in D_i$, performs its processing procedure and decodes its signal to obtain the bitstream of the transmitted signal. The decoded bitstream is then encoded at the achievable rate of the side-channel, which is determined by the SNR on the side-channel, to form the relaying signal. The relaying signal is broadcast by each user in D_i orthogonally, in sequence.

3.2.2 Processing Step

When User k performs its processing step, it will have received decode-and-forward signals from a preceding set of decode-and-forward users, which we denote as D_i^k, in the same way that successive interference cancellation operates. User k first decodes the side-channel signals to obtain the relevant bitstream. Then the user re-encodes and modulates the bitstream to obtain the symbol stream, that is, s_j for $j \in D_i^k$.

After obtaining the symbols, the user then applies the effective channel to the symbols to obtain the interference signals to cancel. For every symbol s_j with $j \in D_i^k$, User k applies the effective channel and scaling to obtain the relevant interference signals $c_{cj}\mathbf{h}_k\mathbf{h}_j^H s_j$.

The interference signals are subtracted from the signal received on the main-channel, which is then normalized to obtain the symbol estimate

$$\begin{aligned}\hat{s}_k &= \frac{y_k - \sum_{j\in D_i^k} c_{cj}\mathbf{h}_k\mathbf{h}_j^H s_j}{\mathbf{h}_k\mathbf{h}_k^H} \\ &= \frac{\sum_{l\in D_i^k} \mathbf{h}_k\mathbf{h}_l^H s_l + n_k - \sum_{j\in D_i^k} \mathbf{h}_k\mathbf{h}_j^H s_j}{\mathbf{h}_k\mathbf{h}_k^H} \\ &= \underbrace{c_{cj}s_k}_{\text{signal}} + \underbrace{\frac{\sum_{l\in U\setminus D_i^k\setminus\{k\}} c_{cj}\mathbf{h}_k\mathbf{h}_l^H s_l}{\mathbf{h}_k\mathbf{h}_k^H}}_{\text{interference}} + \underbrace{\frac{n_k}{\mathbf{h}_k\mathbf{h}_k^H}}_{\text{noise}}.\end{aligned} \tag{3.6}$$

3.3 Cooperative Inter-beam Nulling and Cancellation

Cooperative Inter-beam Nulling and Cancellation (CINC) is the interference management strategy that combines CIN and CIC. The specific details of each step are described in the subsections below, and a diagram of the receiver process is shown in Fig. 3.4.

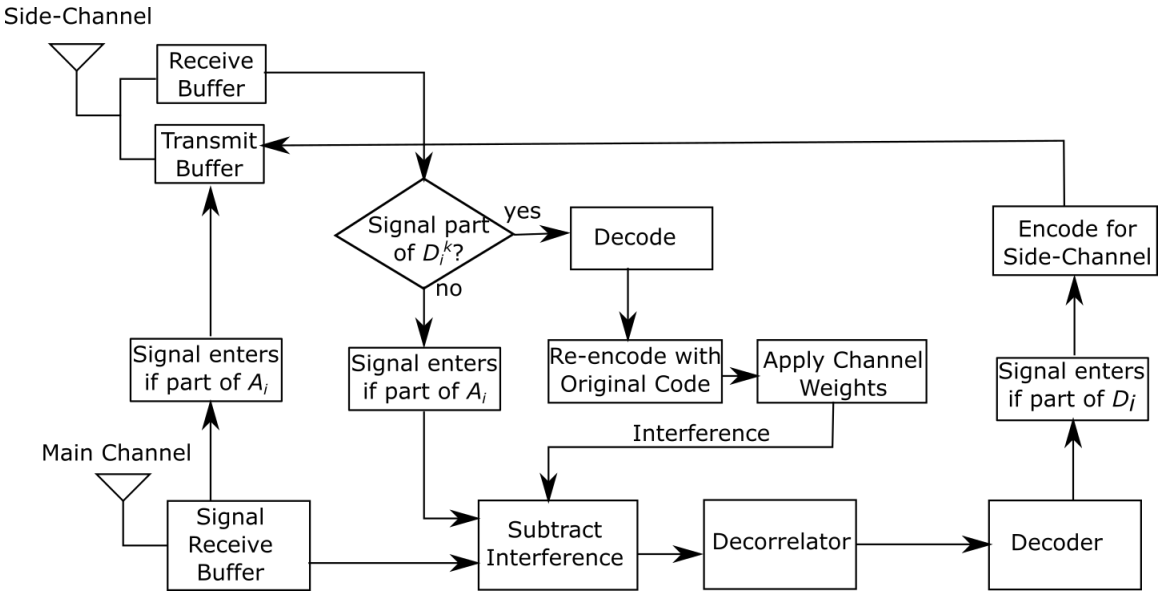

Figure 3.4: CINC User Architecture

3.3.1 Relaying Step

First, users belonging to the amplify-and-forward group A_i broadcast and relay the signals received on the side-channel in the same process as described in the CIN section. Just as in CIN, the received amplify-and-forward signals are normalized. Then, users that are part of the decode-and-forward group D_i perform decode-and-forward relaying in sequence, as described in the CIC section.

3.3.2 Processing Step

First, users perform successive interference cancellation. Just as in CIC, each User k receives the decode-and-forward side-channel signals from the users in D_i^k. The signals are decoded to obtain the bitstream, then re-encoded with the main-channel code and modulated to obtain the original symbols. The effective channel and scaling then is applied to each symbol in order to subtract the interference from both the main-channel signal as well as normalized amplify-and-forward side-channel signals,

resulting in

$$y_k - \sum_{l \in D_i^k} c_{cj} \mathbf{h}_k \mathbf{h}_l^H s_l = \sum_{l \in U \setminus D_i^k} \mathbf{h}_k \mathbf{h}_l^H s_l + n_k$$

for the main-channel signal and

$$y'_{jk} - \sum_{l \in D_i^k} c_{cj} \mathbf{h}_j \mathbf{h}_l^H s_l = \sum_{l \in U \setminus D_i^k} \mathbf{h}_j \mathbf{h}_l^H s_l + n_j + \frac{n_{jk}}{a_j h_{jk}}$$

for the side-channel amplify-and-forward signals that do not belong D_i^k.

After having the interference subtracted, the main-channel and normalized amplify-and-forward side-channel signals are gathered in a signal vector similarly to CIN, with the form

$$\mathbf{Y}_k = c_{cj} \mathbf{H}_k \mathbf{H}_G^H \mathbf{s} + \mathbf{n}_k,$$

, where $\mathbf{Y}_k$ is the column vector containing the main-channel signal y_k and normalized relayed signals y'_{jk} for $j \in A_i \setminus D_i^k \setminus \{k\}$, $\mathbf{H}_k$ is the matrix comprised of the rows $\mathbf{h}_l$ with $l \in A_i \cup \{k\} \setminus D_i^k$, $\mathbf{H}_G$ is the matrix comprised of the rows $\mathbf{h}_l$ with $l \in U \setminus D_i^k$ and $\mathbf{n}_k$ is a column vector containing n_k and $n_j + n_{jk}/(a_j h_{jk})$ for $j \in A_i \setminus D_i^k \setminus \{k\}$.

The decorrelator applied is, as in CIN, the same as equation 3.4. The resultant final symbol estimate is therefore

$$\begin{aligned} \hat{\mathbf{s}}_k &= F_k \mathbf{Y}_\mathbf{k} \\ &= \mathbf{r}_k (\mathbf{H}_k \mathbf{H}_k^H)^{-1} (\mathbf{H}_k \mathbf{H}_G^H \mathbf{s} + \mathbf{n}_k) \\ &= \underbrace{c_{cj} s_k}_{\text{signal}} + \underbrace{c_{cj} \mathbf{r}_k \mathbf{H}_k^{H+} \mathbf{H}_W^H \mathbf{s}_k^c}_{\text{interference}} + \underbrace{\mathbf{r}_k (\mathbf{H}_k \mathbf{H}_k^H)^{-1} \mathbf{n}_k}_{\text{noise}}, \end{aligned} \tag{3.7}$$

where $\mathbf{H}_W$ is comprised of the rows $\mathbf{h}_l$ with $l \in U \setminus A_i \setminus D_i^k \setminus \{k\}$ and $\mathbf{s}_k^c$ is a column vector comprised of the symbols s_l with $l \in U \setminus A_i \setminus D_i^k \setminus \{k\}$.

Chapter 4

Effective SINR in Rayleigh Fading Channels

Based on the symbol estimate formulas we derived for each cooperative strategy in Equations 3.5, 3.6, 3.7, we can compute the resultant effective SINR, which we define to be

$$\text{SINR} = \frac{\mathbb{E}[|\text{signal}|^2]}{\mathbb{E}[|\text{interference}|^2] + \mathbb{E}[|\text{noise}|^2}, \tag{4.1}$$

where the signal, interference, and noise is measured after all processing steps, as noted in Fig. 3.2, 3.3, and 3.4.

We assume Rayleigh fading channels, in which the entries of $\mathbf{H}$ are distributed as $\mathbf{H} \sim CN(0, 1)$, allowing us to compute the expectation in more fundamental terms. The proofs for the following SINR calculations can be found in Appendix A.

The variables used in this section are explained in Section II and Section III of this paper. As a reminder on the key variables used here, A_i is the set of amplify-and-forward relayers, D_i^k is the set of preceding decode-and-forward relayers, M is the number of base station antennas, K is the number of users, P_M is the power budget at the base station, and P_S is the SNR of the side-channel.

We first establish conjugate beamforming as a baseline for comparison. The SINR

calculated is

$$SINR_{cj} = \frac{S_{cj}}{I_{cj} + N_{cj}} \tag{4.2}$$

$$S_{cj} = \frac{P_M}{MK} \tag{4.3}$$

$$I_{cj} = \frac{P_M(K-1)}{MK(M-1)} \tag{4.4}$$

$$N_{cj} = \frac{MN_0}{(M-1)[(M-1)^2-1]} \tag{4.5}$$

A useful metric to examine interference in isolation is the SIR, which is defined to be the SINR when $N_0 = 0$. The SIR for conjugate beamforming is

$$SIR_{cj} = \frac{M-1}{K-1}. \tag{4.6}$$

The SINR achieved by CIN is

$$SINR_{CIN} = \frac{S_{CIN}}{I_{CIN} + N_{CIN}} \tag{4.7}$$

$$S_{CIN} = \frac{P_M}{MK} \tag{4.8}$$

$$I_{CIN} = \frac{P_M(K - |A_i \cup \{k\}|)}{MK(M - |A_i \cup \{k\}|)} \tag{4.9}$$

$$N_{CIN} = \frac{MN_0 + \frac{P_M(M+3)+K}{P_S K} N_{0,s} |A_i \setminus \{k\}|}{(M - |A_i \cup \{k\}|)[(M - |A_i \cup \{k\}|)^2 - 1]} \tag{4.10}$$

The SIR achieved is therefore

$$SIR_{CIN} = \frac{M - |A_i \cup \{k\}|}{K - |A_i \cup \{k\}|}. \tag{4.11}$$

Equation 4.11 tells us how interference is reduced with respect to the number of relayers, where $|A_i|$ is the number of amplify-and-forward relayers. The key point to the SIR equation is that it increases superlinearly with the number of relayers, up to

a maximum of infinite SIR, with zero interference. Each additional relayer improves the SIR for other users by more than the preceding relayers. Assuming that each relayer incurs the same cost, the SIR equation tells us that the most cost-effective point to operate at, that is, the point with the most SIR improvement per relayer, occurs when the number of relayers is maximized.

As a side-remark, we note that increasing the number of base station antennas causes the SIR improvement per relayer to increase. As a result, CIN is well suited for massive MIMO systems.

Equation 4.10 additionally tells us that there is a trade-off for adding relayers: the effective noise is amplified with each additional relayer. However, the noise amplification effect is minimized when the number of base station antennas increases, which again makes the strategies well-suited for massive MIMO systems.

The SINR achieved by CIC is

$$SINR_{CIC} = \frac{S_{CIC}}{I_{CIC} + N_{CIC}} \tag{4.12}$$

$$S_{CIC} = \frac{P_M}{MK} \tag{4.13}$$

$$I_{CIC} = \frac{P_M(K - |D_i^k \cup \{k\}|)}{MK(M-1)} \tag{4.14}$$

$$N_{CIC} = \frac{MN_0}{(M-1)[(M-1)^2 - 1]}. \tag{4.15}$$

The SIR achieved is therefore

$$SIR_{CIC} = \frac{M-1}{K - |D_i^k \cup \{k\}|}. \tag{4.16}$$

At this point, we would like to remind the reader that D_i^k refers to the set of preceding decode-and-forward users.

The SIR achieved by CIC has a similar form to the SIR achieved by CIN. Both

provide the benefitting users with a superlinear improvement in SIR. However, unlike CIN, CIC provides a greater SIR improvement for benefitting users, as evidenced by the $M-1$ term in the numerator in Equation 4.16 compared to the $M-|A_i|$ term for CIN in Equation 4.11. The caveat to the greater SIR improvement is that a smaller subset of users achieves the full benefit for the same number of relayers; a user only benefits from preceding relayers.

Another point of difference is that the noise term for CIC in Equation 4.15 is not amplified when the number of relayers increases. CIC is therefore the better option when the interference-to-noise ratio is relatively low, and when the number of base station antennas, which affects the amount of noise amplification for CIN, is low.

Finally, the SINR achieved by CINC is

$$SINR_{CINC} = \frac{S_{CINC}}{I_{CINC} + N_{CINC}} \tag{4.17}$$

$$S_{CINC} = \frac{P_M}{MK} \tag{4.18}$$

$$I_{CINC} = \frac{P_M(K - |D_i^k \cup A_i \cup \{k\}|)}{MK(M - |A_i \cup \{k\} \setminus D_i^k|)} \tag{4.19}$$

$$N_{CINC} = \frac{MN_0 + \frac{P_M(M+3)+K}{P_S K} N_{0,s}|A_i \setminus D_i^k \setminus \{k\}|}{(M - |A_i \setminus D_i^k \cup \{k\}|)[(M - |A_i \setminus D_i^k \cup \{k\}|)^2 - 1]}. \tag{4.20}$$

The SIR achieved is therefore

$$SIR_{CINC} = \frac{M - |A_i \cup \{k\} \setminus D_i^k|}{K - |D_i^k \cup A_i \cup \{k\}|} \tag{4.21}$$

Equations 4.20 and 4.21 combine the insights provided by CIN and CIC for each type of relayer. The additional point of insight is in examining the effect of relayers in both A_i and D_i, that is, relayers that perform both amplify-and-forward and decode-and-forward relaying. From Equation 4.21, each additional *unique* relayer provides superlinear improvement through the $K - |D_i^k \cup A_i \cup \{k\}|$ denominator. However, an

additional decode-and-forward relay from a user that has already performed amplify-and-forward relaying only provides a linear improvement in the $M - |A_i \cup \{k\} \setminus D_i^k|$ numerator.

Chapter 5

Simulation Results

In our simulations, we examine the effect of limited side-channel resources on the achievable sum-rate of the system. More specifically, we look at the time-bandwidth costs as well as the power costs needed to achieve a certain sum-rate performance for each strategy. In the process of examining the sum-rate, we obtain insight into which situations are better for cancellation and which situations are better for nulling, the optimal relaying assignments for CINC, and the level of improvement the proposed cooperative methods can achieve.

In this work, we define achievable sum-rate to be $R_{sum} = \sum_{i \in U} \log_2(1 + \text{SINR}_i)$, where the SINR expressions are those computed in the previous section.

5.1 Modeling Limited Side-channel Resources

We assume that the orthogonal side-channel has limited time and bandwidth resources to dedicate to interference reduction. We define the time-bandwidth resources available on the side-channel for interference reduction per block to be $(WT)_{side}$, and we define β to be the ratio between time-bandwidth resources dedicated to the side-channel per transmit block and the time-bandwidth resources on the main channel in

a transmit block, that is,

$$\beta = \frac{(WT)_{side}}{(WT)_{main}}. \tag{5.1}$$

In CIN, amplify-and-forward is used, which indicates that there is a one-to-one correspondence between each symbol time for the main channel and the side-channel. The one-to-one correspondence implies a constraint given a certain amount of time-bandwidth resources, namely,

$$|A_i|(WT)_{main} \leq (WT)_{side},$$

where the left side of the inequality represents the amount of symbol time consumed on the side-channel for a given number of broadcasters, and the right side of the inequality represents the total amount of effective side-channel symbol times available. We can isolate the number of broadcasters in the inequality to simplify, giving

$$|A_i| \leq \beta.$$

In CIC, decode-and-forward is used, which indicates that rather than a one-to-one correspondence between each symbol time, there is a one-to-one correspondence in the number of bits transmitted on the main channel compared to the side-channel. We assume that all transmissions occur at the $\log_2(1 + \text{SINR})$ achievable rate, at which users can theoretically perform nearly error-free decoding. Finding the number of bits that could be transmitted in the main channel and the side-channel is dependent only on the achievable rates and the time-bandwidth resources on the main channel and on the side-channel, giving the inequality

$$\sum_{i \in D_i} (WT)_{main} R_i \leq (WT)_{side} R_{side}.$$

The left side of the above inequality represents the number of bits that need to be sent to accommodate a given broadcasting group, while the right side of the inequality represents the total number of bits that the side-channel can accommodate. We can rearrange and expand the terms in the inequality to find

$$\sum_{i \in D_i} \log_2(1 + \mathrm{SINR}_i) \leq \beta \log_2(1 + \mathrm{SNR}_{sc}),$$

which gives us the information needed to determine the size of the broadcasting group.

CINC has both amplify-and-forward decode-and-forward relaying, which combines the previous two restrictions. There is both the one-to-one correspondence in symbol-time for each amplify-and-forward relayer as well as a one-to-one bit correspondence for each decode-and-forward relayer, yielding

$$|A_i| + \sum_{i \in D_i} \frac{\log_2(1 + \mathrm{SINR}_i)}{\log_2(1 + \mathrm{SNR}_{sc})} \leq \beta.$$

5.2 Rayleigh Channel Simulations

Unless otherwise specified, the default parameters of our simulation are: $P_M = 20$dB over the noise floor, $M = 100$ base-station antennas, $K = 8$ users, side-channel SNR = 20dB. We assume that the cooperation group comprises all users in the system. We perform two simulations. Our first simulation is used to examine the level of improvement that can be expected from the proposed strategies. An SNR of 20dB is chosen as a representative value because it is often considered the minimum SNR for a data link in WLAN systems.

For CINC simulations, we perform an exhaustive search of every possible combination of amplify-and-forward relayers and decode-and-forward relayers. We find the combination of amplify-and-forward and decode-and-forward relayers that achieves

the greatest sum rate to determine the optimal distribution of relayers.

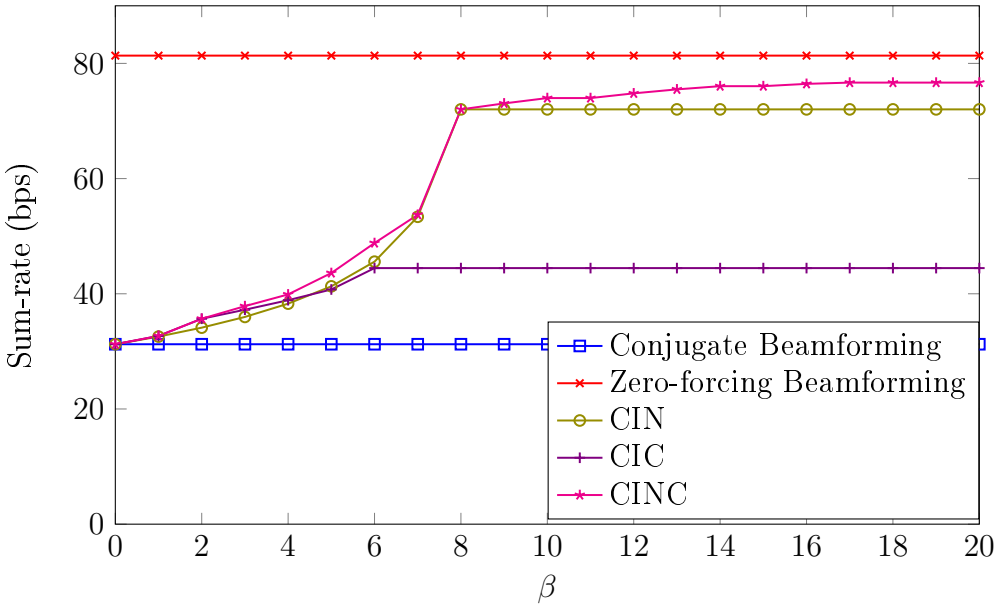

Figure 5.1: Sum-rate of cooperative strategies with respect to β.

Our first simulation generated the plots in Figures 5.1, 5.2, and 5.3. Figure 5.1 shows the sum-rate with different strategies. Figure 5.2 shows the corresponding number of relayers associated with each β for this simulation. Finally, Figure 5.3 shows the percent improvement from each cooperative strategy. As stated before, the first simulation is meant to show the level of improvement that can be expected from each strategy.

As we can see from Figure 5.1, CINC is capable of approaching the level of performance of zero-forcing beamforming. The sum-rate increases at a much higher rate for β values between 0 and K, then level off to increase at a much lower rate for $\beta > 8$.

CIC, on the other hand, peaks at a much lower sum-rate than CINC and CIN, but achieves a higher sum-rate for the range $1 < \beta < 6$. The reason for the higher sum-rate in this β range can be seen in Fig. 5.2, where we see that CIC can support a greater number of relayers for the same amount of time-bandwidth resources in that range. However, the reason that CIC peaks at a lower rate is because successive

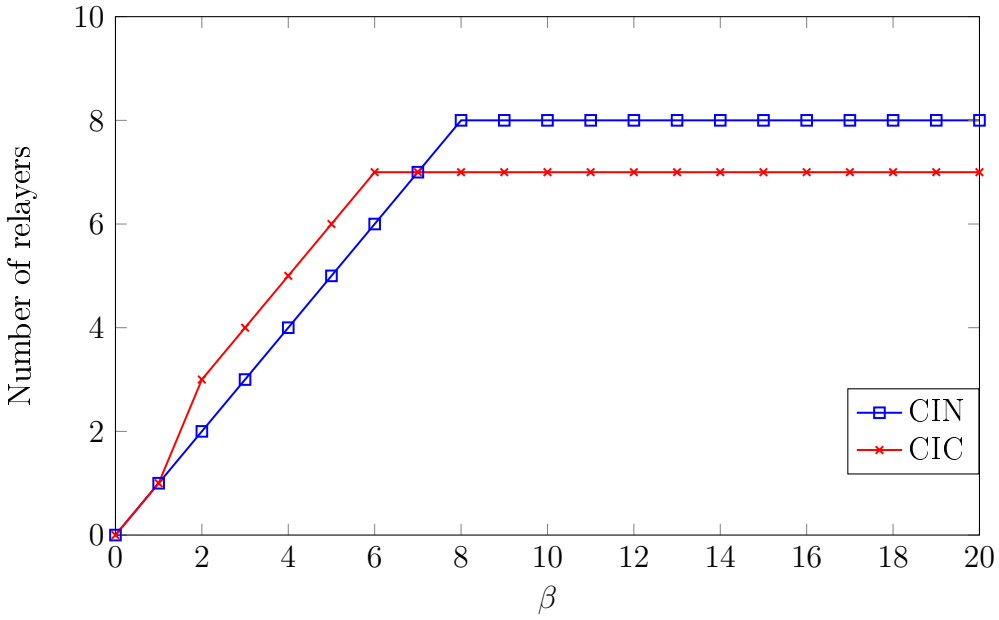

Figure 5.2: Number of CIN and CIC relayers with respect to β.

interference cancellation does not benefit a large subset of users, while the decorrelator in CIN and CINC benefits all the users except the relayers.

The resultant improvement can be found in Fig. 5.3. We see that at a high β value, $\beta = 12$, CIN and CINC achieves over double the sum-rate of conjugate beamforming only, with percentage improvement at 130 % for CIN and 139 % for CINC. Meanwhile, CIC achieves a modest performance improvement of 42% at $\beta = 12$.

Even for low amounts of side-channel time-bandwidth resources, for example at $\beta = 3$, cooperative strategies can still achieve significant sum-rate improvement. At $\beta = 3$, CINC achieves 21 % improvement, CIN achieves 15 % improvement, and CIC achieves 19% improvement in sum-rate over conjugate beamforming only systems.

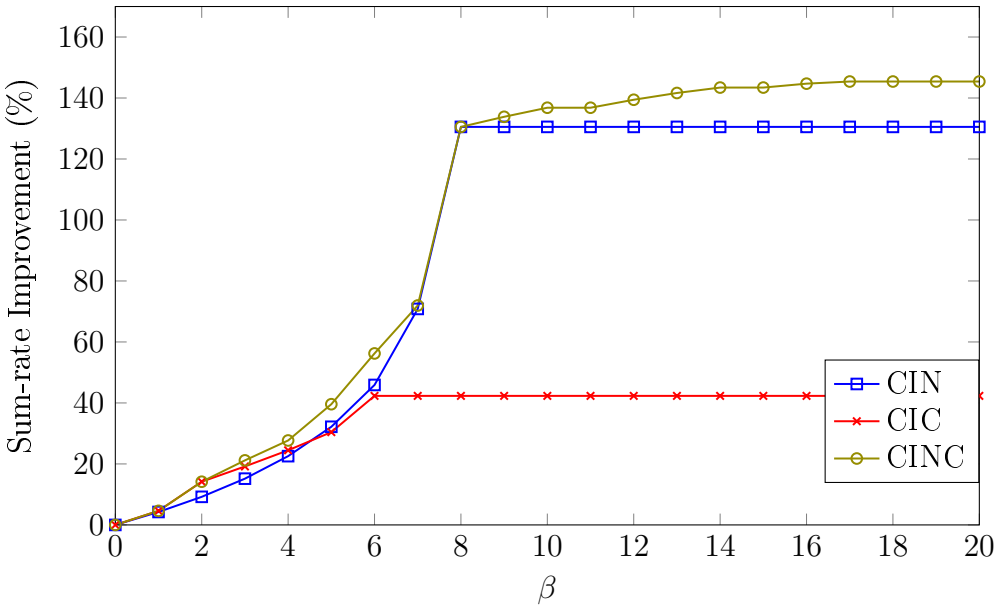

Figure 5.3: Percentage sum-rate improvement over conjugate beamforming with respect to β.

Our second simulation generated the plot in Figure 5.4. The figure depicts the 8-user, 100-antenna scenario with full cooperation, in which every user relays its signal, and sweeps over side-channel SNR.

The key observation in Figure 5.4 is that cooperative strategies only start to improve over conjugate beamforming performance after side-channel SNR exceeds approximately 0 dB. At values less than 0 dB, cooperative strategies do not provide significant (> 10 %) improvement because the noise from the side-channel makes cooperation much less useful.

Our third simulation generated the plot in Figure 5.5. The figure depicts the 8-user, 100-antenna scenario with full cooperation and side-channel SNR equal to 20 dB, and sweeps over main channel SNR.

The key observation in Figure 5.5 is that, similarly to side-channel SNR, cooperative strategies only start to improve over conjugate beamforming performance after side-channel SNR exceeds approximately 0 dB. At values less than 0 dB, cooperative

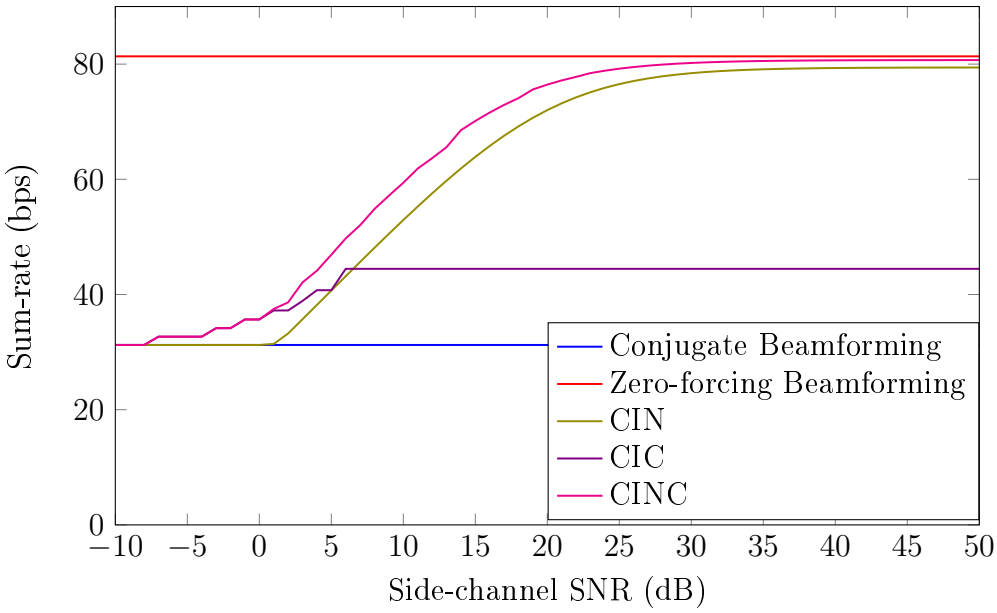

Figure 5.4: Sum rate of cooperative strategies with respect to side-channel SNR.

strategies do not provide significant (> 10 %) improvement because the system is primarily noise-limited rather than interference limited. At main channel SNR greater than 20 dB, the improvement from cooperative strategies levels out because at that point, side-channel SNR, which is at 20 dB, becomes the main bottleneck.

Our fourth simulation generated the plot in Figure 5.6. The figure depicts the 100-antenna scenario with full cooperation and side-channel SNR equal to 20 dB and sweeps over possible numbers of users.

The key observation in Figure 5.6 is that the gap between conjugate beamforming and the cooperative strategies tends to grow as the number of users increases. As the number of users increases, there are increasing sources of interference that the cooperative strategies can improve on.

Our fifth simulation generated the plot in Figure 5.7, and it examines the case where there's limited time-bandwidth ($\beta = 4$), but increasing numbers of users. The simulation examines what happens when the ratio of relayers to users decreases.

The key observation is that it reaches a local maximum where there is full cooper-

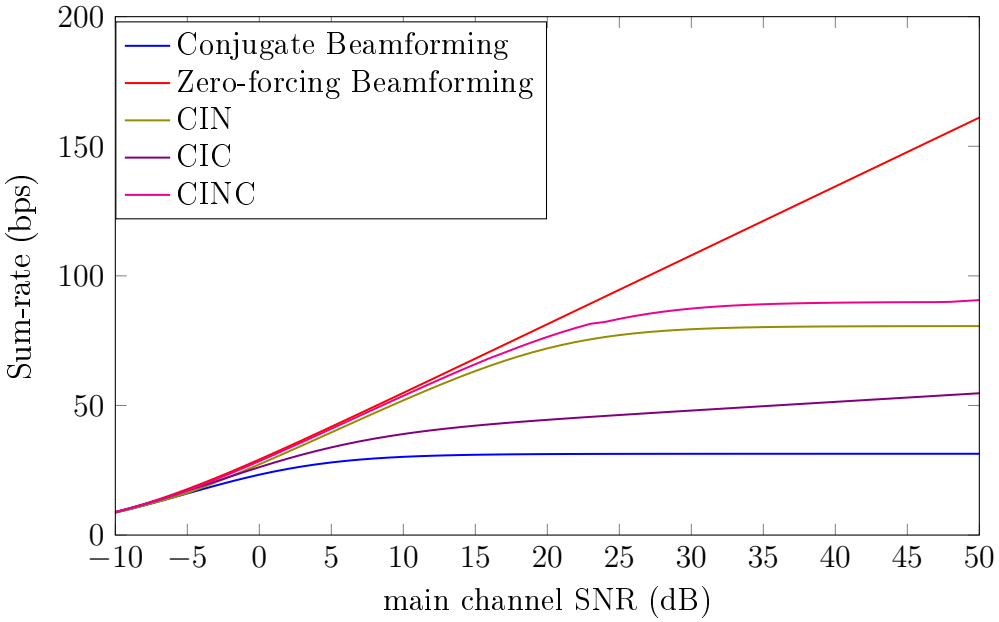

Figure 5.5: Sum rate of cooperative strategies with respect to main channel SNR.

ation, after which nulling contributes little compared to cancellation. As the number of users increases and the number of relayers stays the same, cancellation performs better simply because a greater fraction of the users get the increased benefit of cancellation.

Our sixth simulation generated the plot in Figure 5.8, and it examines the case where our 8 users are split into two cooperation groups of size 4 each.

The key observation is that having two separate groups severely diminishes the maximum level of improvement that can be achieved with each strategy. Having multiple cooperation groups ensures that there can never be the case where all interferers are dealt with.

Our seventh simulation generated the plot in Figure 5.9. The figure depicts the 8-user scenario with full cooperation and side-channel SNR equal to 20 dB, and sweeps over possible numbers of base station antennas.

The key observation in Figure 5.9 is that the gap between conjugate beamforming

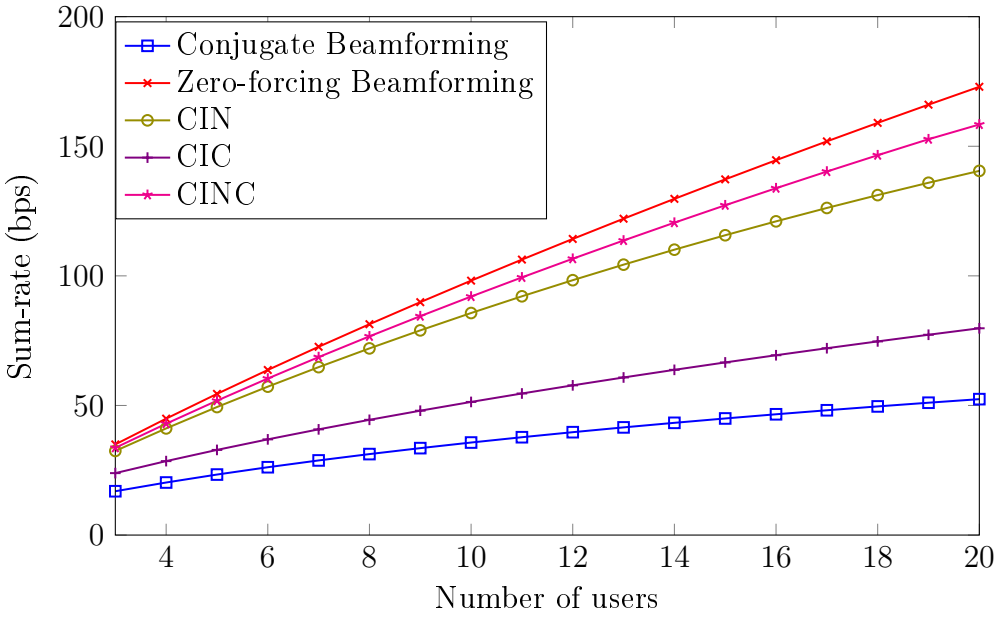

Figure 5.6: Sum rate of cooperative strategies with respect to number of users.

and the cooperative strategies that include nulling tends to grow as the number of base station antennas increases. As the number of base station antennas increases, the observation from Equation 4.11 continues to hold: the rate at which SIR improves becomes greater as the number of base station antennas grows.

Our final simulation generates the plot found in Fig. 5.10. We simulate across a grid of side-channel SNR and β values to determine the allocation of relayers that results in the greatest sum-rate. The optimal allocation is found by performing an exhaustive search over every combination of amplify-and-forward and decode-and-forward relayers.

The plot describes regimes at which the optimal distribution of relayers for CINC should contain more amplify-and-forward relayers or more decode-and-forward relayers. The plot can be understood as follows: in the blue regions, side-channel resources should be prioritized for amplify-and-forward relayers; in the red regions, side-channel resources should be prioritized for decode-and-forward relayers; in the yellow regions, both should be prioritized equally. We find that there are three main regimes at

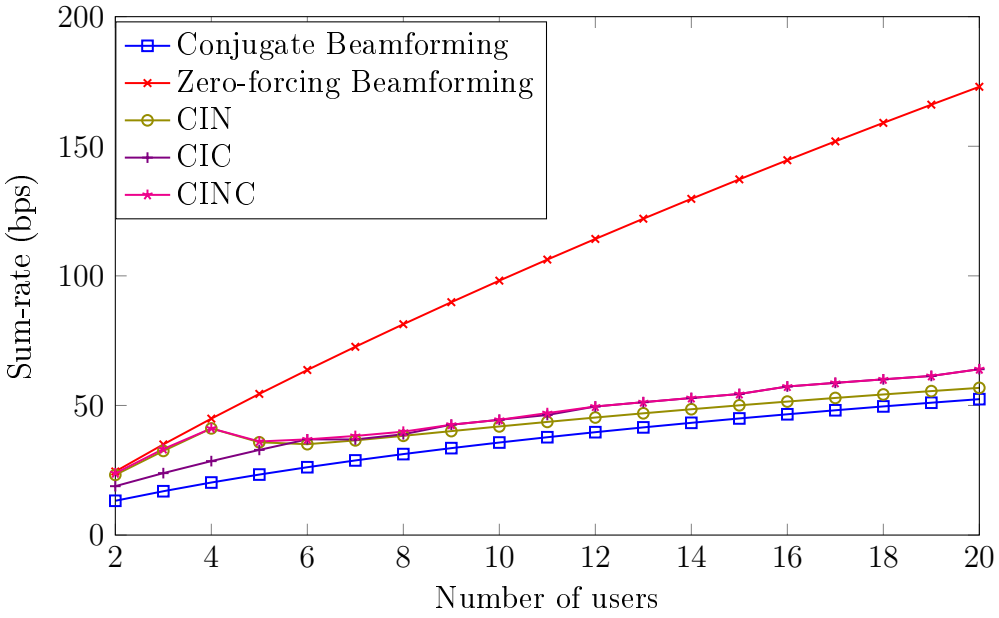

Figure 5.7: Sum rate of cooperative strategies with respect to number of users.

which different types of relayers should be prioritized.

The first regime is at side-channel SNR $< 5dB$, at which decode-and-forward should be prioritized. In the first regime, amplify-and-forward causes an amplification of noise when side-channel noise is significant, as discussed in Section 4. Decode-and-forward does not amplify noise, and therefore should be prioritized.

The second regime is at a side-channel SNR $> 20dB$, and $\beta \leq 7$, at which decode-and-forward should be prioritized. In the second regime, each time-bandwidth block can accommodate multiple decode-and-forward relayers due to the high SNR, but only a single amplify-and-forward relayer. As a result, decode-and-forward is prioritized in the second regime.

The third regime comprises of every other combination of side-channel SNR and β values, at which amplify-and-forward relayers are prioritized. Amplify-and-forward relayers are prioritized in the third regime because while they provide less interference reduction and suffer from a noise trade-off, as discussed in Section 4, amplify-and-forward relayers provide benefit to a greater number of users. Decode-and-forward

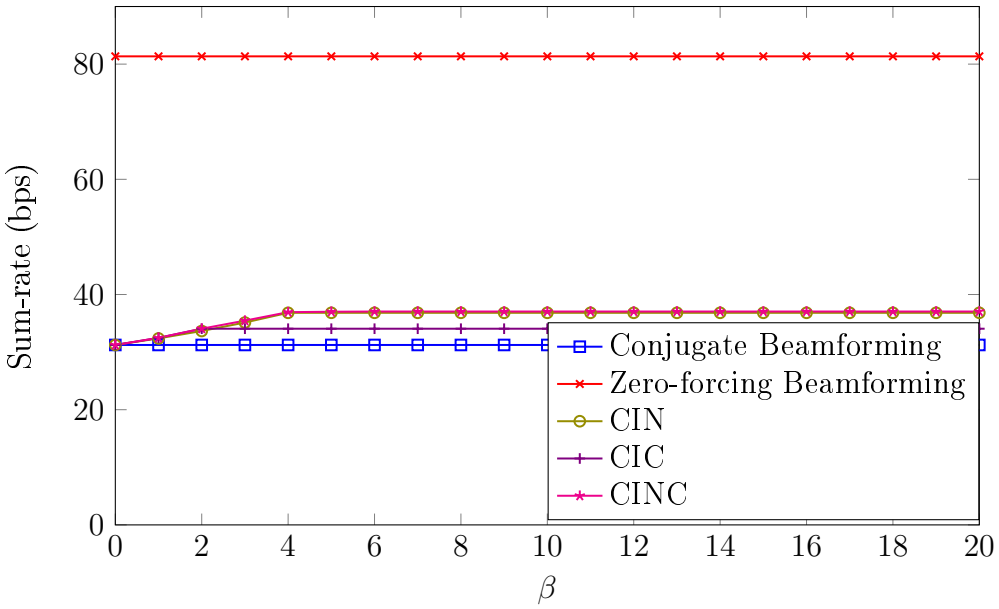

Figure 5.8: Sum-rate of cooperative strategies with respect to β.

relayers only provide benefit to subsequent users, which is a smaller subset, especially as the number of decode-and-forward relayers increases. Therefore, amplify-and-forward relayers should be prioritized in the third regime, especially as β values increase.

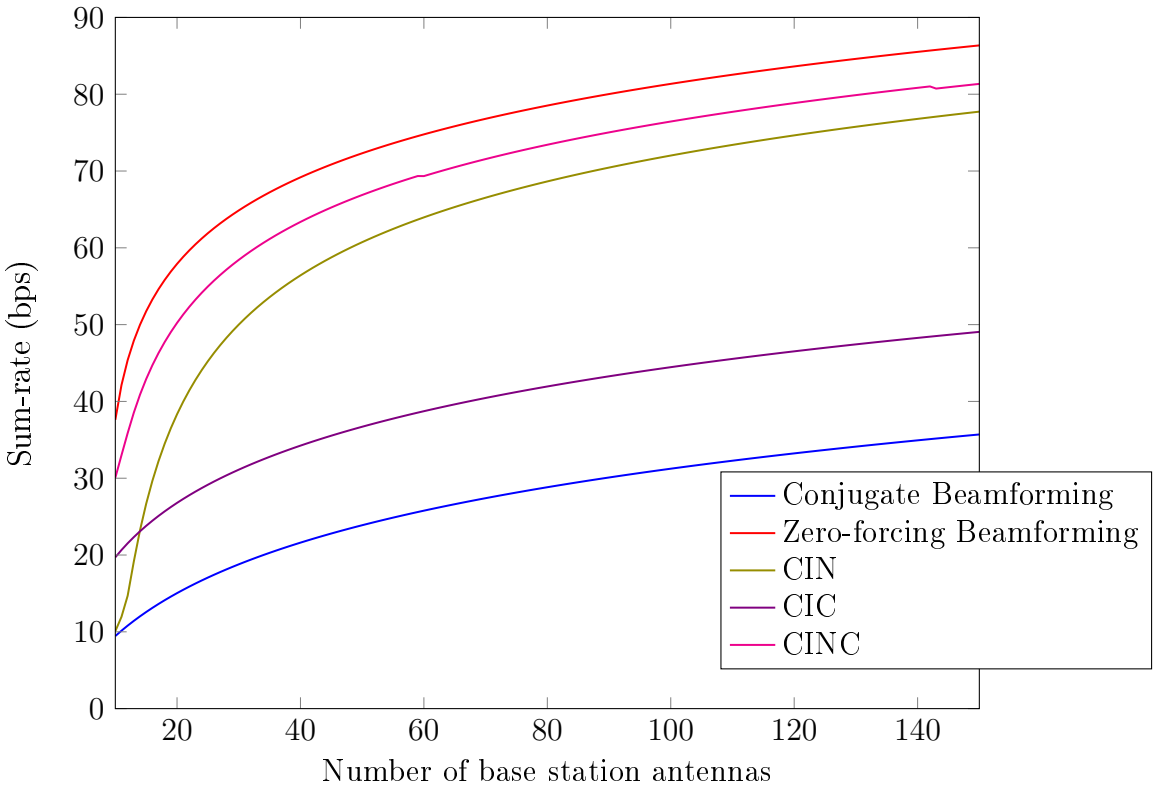

Figure 5.9: Sum rate of cooperative strategies with respect to number of base station antennas.

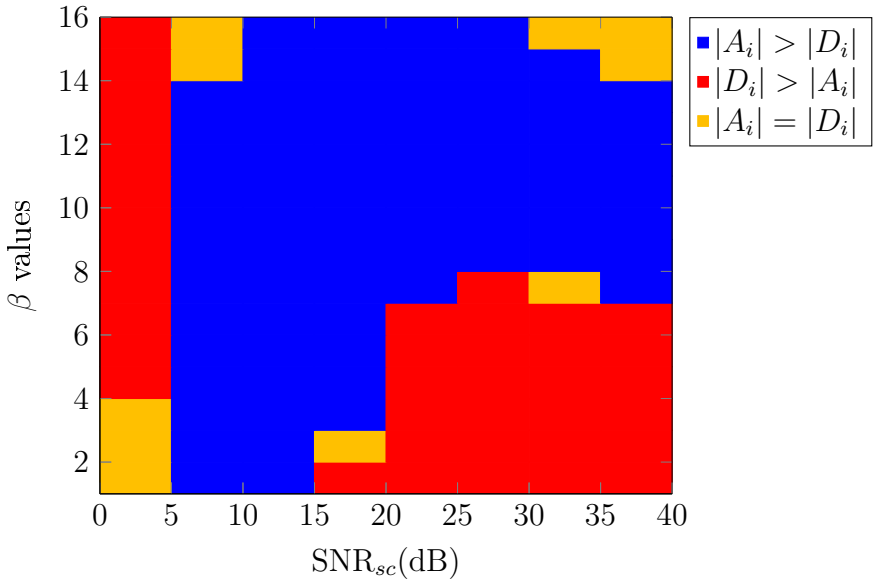

Figure 5.10: Relayer Type Priority Map for CINC

Chapter 6

Conclusion

We proposed three cooperative strategies for managing inter-beam interference using side-channels in a conjugate beamforming, massive MIMO system. The three strategies are based on enabling V-BLAST and its respective components over side-channels rather than wired channels: the first, CIN, uses amplify-and-forward relaying to enable the decorrelator portion of V-BLAST; the second, CIC, uses decode-and-forward relaying to enable the SIC portion of V-BLAST; and the third, CINC, contains the full V-BLAST system over side-channels;.

Unlike previous works, we study the cooperative strategies under the paradigm of limited side-channel power and time-bandwidth, which limits the number of relayers that the strategies can support. We develop insights on how much improvement can be expected for a given amount of side-channel resources, and how resources should be allocated to each type of relayer when we know the amount of side-channel resources available

We find that when there are enough resources for all users to relay, CIN experiences a sum-rate percentage improvement of 130 %, CINC of 139 %, and CIC of 42%. When time-bandwidth resources are limited to 3 times the amount on the main-channel, CIN experiences a sum-rate percentage improvement of 15 %, CINC of 21 %, and CIC of

19%.

Finally, we outline regimes at which different types of relaying should be prioritized in a CINC system. Amplify-and-forward relaying should be prioritized in general, except when side-channel SNR is less than 5 dB and when side-channel SNR is greater than 20 dB with time-bandwidth resources on the side-channel limited to less than the number of users times the time-bandwidth on the main-channel.

Appendix A

Effective SINR Computations

For a user in cooperation group C_i, which we denote as User k, the symbol estimate received is found in Equation 3.5, 3.6, and 3.7. We find the power of the signal, interference, and noise terms individually for each strategy.

A.1 Signal Power

We start with the signal term for CIN, found in Equation 3.5,

$$\begin{aligned}\mathbb{E}[|\text{signal}|^2_{CIN}] &= \mathbb{E}[|c_{cj}s_k|^2] \\ &= |c_{cj}|^2. \end{aligned} \tag{A.1}$$

Our model has an average power constraint such that

$$c_{cj} = \sqrt{\frac{P_M}{\mathbb{E}[\text{Tr}(\mathbf{H}\mathbf{H}^H)]}},$$

as shown in Equation 2.2.

$\mathbf{H}$ is a $K \times M$ Gaussian uncorrelated matrix for Rayleigh fading, for which we

find that

$$\mathbb{E}[\mathrm{Tr}(\mathbf{H}\mathbf{H}^H)] = MK. \tag{A.2}$$

Therefore, combining A.1, 2.2, and A.2, we find that

$$\mathbb{E}[|\mathrm{signal}|^2_{CIN}] = \frac{P_M}{MK}. \tag{A.3}$$

We note that due to the normalization, each strategy, including conjugate beamforming only, has the same signal power. Therefore, we can generalize Equation A.3 to find that

$$\mathbb{E}[|\mathrm{signal}|^2] = \frac{P_M}{MK}. \tag{A.4}$$

A.2 Interference Power

From Equation 3.5, the variance of the interference term can be expressed as

$$\begin{aligned}\mathbb{E}[|\mathrm{interference}|^2_{CIN}] &= c_{cj}^2 \mathbb{E}[|\mathbf{r}_k \mathbf{H}_k^+ \mathbf{H}_{k,F}^H \mathbf{s}_k^c|^2] \\ &= c_{cj}^2 \mathbb{E}[\bar{\mathbf{h}}_k \mathbf{H}_{k,F}^H \mathbf{H}_{k,F} \bar{\mathbf{h}}_k^H],\end{aligned} \tag{A.5}$$

where $\bar{\mathbf{h}}_k = \mathbf{r}_k \mathbf{H}_k^+$, which is simply the $1 \times M$ row of the pseudoinverse that corresponds to User k.

The interference term equations are in quadratic form and can thus be expanded

to

$$\begin{aligned}\mathbb{E}[|\text{interference}|^2_{CIN}] &= c_{cj}^2 \mathbb{E}[\bar{\mathbf{h}}_k \mathbf{H}_{k,F}^H \mathbf{H}_{k,F} \bar{\mathbf{h}}_k^H] \\ &= c_{cj}^2 \mathbb{E}\left[\sum_{i=1}^{M}\sum_{j=1}^{M} \bar{h}_{ik}\bar{h}_{jk}^* (\mathbf{H}_{k,F}^H \mathbf{H}_{k,F})_{ij}\right] \\ &= c_{cj}^2 \sum_{i=1}^{M} \mathbb{E}[\bar{h}_{ik}\bar{h}_{ik}^* (\mathbf{H}_{k,F}^H \mathbf{H}_{k,F})_{ii}] \\ &= c_{cj}^2 \sum_{i=1}^{M} \mathbb{E}[\bar{h}_{ik}\bar{h}_{ik}^*]\mathbb{E}[(\mathbf{H}_{k,F}^H \mathbf{H}_{k,F})_{ii}]. \end{aligned} \tag{A.6}$$

The third step in Equation A.6 is found by noting that $(\mathbf{H}_{k,F}^H \mathbf{H}_{k,F})_{ij} = 0 \quad \forall \quad i \neq j$. The fourth step is found by noting that $\bar{h}_{ik}$ and $(\mathbf{H}_{k,F}^H \mathbf{H}_{k,F})_{ii}$ are independent.

$(\mathbf{H}_{k,F}^H \mathbf{H}_{k,F})_{ii}$ is simply the inner product of the i-th row of the Rayleigh matrix with itself. We know that $\mathbf{H}_{k,F}$ is a $K - |A_i \cup \{k\}| \times M$ Gaussian matrix, which allows to simply find that

$$\mathbb{E}[(\mathbf{H}_{k,F}^H \mathbf{H}_{k,F})_{ii}] = K - |A_i \cup \{k\}|. \tag{A.7}$$

The pseudoinverse moments of a complex Gaussian matrix can be found in Example 4.1 of [12], which, combined with the fact that $\mathbf{H}_k$ is a $|A_i \cup \{k\}| \times M$ matrix, allows us to find that

$$\mathbb{E}[\bar{h}_{ik}\bar{h}_{ik}^*] = \frac{1}{M(M - |A_i \cup \{k\}|)}. \tag{A.8}$$

Combining equations A.6, A.7, A.8, and 2.2 allows us to derive

$$\mathbb{E}[|\text{interference}|^2_{CIN}] = \frac{P_M(K - |A_i \cup \{k\}|)}{MK(M - |A_i \cup \{k\}|)}. \tag{A.9}$$

The interference power for conjugate beamforming is an extension of this; however, $\mathbf{H}_k$ for the conjugate beamforming case is a $1 \times M$ matrix, and $\mathbf{H}_{k,F}$ is a $K - 1 \times M$

matrix. Since this is the case, we replace the instances of $|A_i \cup \{k\}|$ with 1, which yields

$$\mathbb{E}[|\text{interference}|^2_{cj}] = \frac{P_M(K-1)}{MK(M-1)}, \tag{A.10}$$

The interference power for CIC is another extension of the CIN case in which $\mathbf{H}_k$ is a $1 \times M$ matrix, but $\mathbf{H}_{k,F}$ is a $K - |D_i^k \cup \{k\}| \times M$ matrix, such that

$$\mathbb{E}[|\text{interference}|^2_{CIC}] = \frac{P_M(K - |D_i^k \cup \{k\}|)}{MK(M-1)}. \tag{A.11}$$

The interference power for CINC follows a similar derivation, with $\mathbf{H}_k$ as a $|A_i \cup \{k\} \setminus D_i^k| \times M$ matrix, but $\mathbf{H}_{k,W}$ is a $K - |D_i^k \cup A_i \cup \{k\}| \times M$ matrix, such that

$$\mathbb{E}[|\text{interference}|^2_{CINC}] = \frac{P_M(K - |D_i^k \cup A_i \cup \{k\}|)}{MK(M - |A_i \cup \{k\} \setminus D_i^k|)}. \tag{A.12}$$

A.3 Noise Power

We examine the noise power for CIN through the symbol estimate in Equation 3.5,

$$\begin{aligned}
\mathbb{E}[|\text{noise}|^2_{CIN}] &= \mathbb{E}[|\mathbf{r}_k(\mathbf{H}_k\mathbf{H}_k^H)^{-1}\mathbf{n}_k|^2] \\
&= \mathbb{E}[\mathbf{h}_k^- \mathbf{n}_k \mathbf{n}_k^H \mathbf{h}_k^{-H}] \\
&= \mathbb{E}[|h_{kk}^-|^2]\mathbb{E}[|n_k|^2] + \sum_{i \in A_i \setminus k} \mathbb{E}[|h_{ik}^-|^2]\mathbb{E}[|n_i|^2]\mathbb{E}\left[\left|\frac{n_{i,s}}{h_{ak}a_i}\right|^2\right]
\end{aligned} \tag{A.13}$$

where $\mathbf{h}_k^-$ is the $1 \times |A_i \cup \{k\}|$ row vector $\mathbf{r}_k(\mathbf{H}_k\mathbf{H}_k^H)^{-1}$, h_{ik}^- is the i-th element of $\mathbf{h}_k^-$, and the noise terms are found by examining Equation 3.3, which tells us that

$$\mathbf{n}_k = \begin{bmatrix} n_a + \frac{n_{a,s}}{h_{ak}a_a} \\ n_b + \frac{n_{b,s}}{h_{bk}a_b} \\ \cdots \\ n_k \\ \cdots \\ n_c + \frac{n_{c,s}}{h_{ck}a_c} \\ n_d + \frac{n_{d,s}}{h_{dk}a_d} \end{bmatrix}, \tag{A.14}$$

where $a, b, c, d \in A_i \cup \{k\} \setminus \{k\}$ and n_k is on the row corresponding to user k.

We also recall in our system model that the amplification factor a is chosen such that the total average received power for each side-channel link is P_S. Therefore,

$$|h_{jk}a_j|^2\mathbb{E}[|y_j|^2] = P_S. \tag{A.15}$$

We see that this term depends on the average received power on the main channel, which can be derived as

$$\begin{aligned} \mathbb{E}[|y_j|^2] &= \mathbb{E}[c_{cj}^2\mathbf{h}_j\mathbf{H}^H\mathbf{H}\mathbf{h}_j^H + |n_j|^2] \\ &= \frac{P_M(M^2+3M)}{MK} + 1, \end{aligned} \tag{A.16}$$

which is found through a tedious application of Isserlis' theorem for complex Gaussian random variables.

Combining Equations A.15 and A.16 allows us to rewrite the side-channel noise

terms in Equation A.14 as

$$\mathbb{E}\left[\left|\frac{n_{a,s}}{h_{ak}a_a}\right|^2\right] = \frac{P_M(M+3)+K}{P_S K}N_{0,s}, \tag{A.17}$$

which gives enough information for the analysis of the $\mathbf{n}_k$ part of equation 15.

Next, we examine the inverse term $\mathbb{E}[\mathbf{h}_k^{-}\mathbf{h}_k^{-H}]$. We start with

$$\mathbb{E}[W^{ij}\Sigma^{lk*}] = \mathbb{E}[\mathrm{Re}W^{ij}\mathrm{Re}\Sigma^{lk} + \mathrm{Im}W^{ij}\mathrm{Im}\Sigma^{lk} + j(-\mathrm{Re}W^{ij}\mathrm{Im}\Sigma^{lk} + \mathrm{Im}W^{ij}\mathrm{Re}\Sigma^{lk})], \tag{A.18}$$

in which W^{ij} is the ij-th element of a Wishart matrix formed from a $L \times M$ Gaussian matrix, with the associated correlation matrix Σ, whose lk-th element is denoted by Σ^{lk}.

Combined with Equations 33-37 in [13], we find that

$$\mathbb{E}[W^{ij}\Sigma^{lk*}] = (M-L)\mathbb{E}[W^{ij}W^{lk*}] - \mathbb{E}[W^{il}W^{kj}]. \tag{A.19}$$

Equations 39, 42, and 43 in [13] can be applied to the above equation to find that

$$\mathbb{E}[W^{ij}W^{lk*}] = \frac{(M-L)\Sigma^{ij}\Sigma^{lk*} + \Sigma^{il}\Sigma^{kj}}{(M-L)[(M-L)^2-1]} \tag{A.20}$$

$$= \frac{(M-L)\Sigma^{ij}\Sigma^{lk*} + \Sigma^{il}\Sigma^{kj}}{(M-L)^3} + O\left(\frac{1}{(M-L)^5}\right) \tag{A.21}$$

$$\approx \frac{(M-L)\Sigma^{ij}\Sigma^{lk*} + \Sigma^{il}\Sigma^{kj}}{(M-L)^3}. \tag{A.22}$$

Applied to our case with $\mathbf{h}_k^{-}$, which is the inverse of the Wishart matrix formed

from the $|A_i \cup \{k\}| \times M$ Gaussian matrix $\mathbf{H}_k$, we find that

$$\mathbb{E}[|h_{kk}^-|^2] = \frac{M - |A_i \cup \{k\}| + 1}{(M - |A_i \cup \{k\}|)[(M - |A_i \cup \{k\}|)^2 - 1]} \tag{A.23}$$

$$= \frac{M - |A_i \cup \{k\}| + 1}{(M - |A_i \cup \{k\}|)^3} + O\left(\frac{1}{(M - |A_i \cup \{k\}|)^5}\right) \tag{A.24}$$

$$\approx \frac{M - |A_i \cup \{k\}| + 1}{(M - |A_i \cup \{k\}|)^3}. \tag{A.25}$$

For the case of $h_i k^-$ when $i \neq k$,

$$\mathbb{E}[|h_{ik}^-|^2] = \frac{1}{(M - |A_i \cup \{k\}|)[(M - |A_i \cup \{k\}|)^2 - 1]} \tag{A.26}$$

$$= \frac{1}{(M - |A_i \cup \{k\}|)^3} + O\left(\frac{1}{(M - |A_i \cup \{k\}|)^5}\right) \tag{A.27}$$

$$\approx \frac{1}{(M - |A_i \cup \{k\}|)^3}. \tag{A.28}$$

Putting together Equations A.26, A.23, A.17, and A.13, we find that

$$\mathbb{E}[|\text{noise}|^2_{CIN}] = \frac{MN_0 + \frac{P_M(M+3)+K}{P_S K} N_{0,s} |A_i \setminus \{k\}|}{(M - |A_i \cup \{k\}|)[(M - |A_i \cup \{k\}|)^2 - 1]} \tag{A.29}$$

$$= \frac{MN_0 + \frac{P_M(M+3)+K}{P_S K} N_{0,s} |A_i \setminus \{k\}|}{(M - |A_i \cup \{k\}|)^3} + O\left(\frac{1}{(M - |A_i \cup \{k\}|)^5}\right) \tag{A.30}$$

$$\approx \frac{MN_0 + \frac{P_M(M+3)+K}{P_S K} N_{0,s} |A_i \setminus \{k\}|}{(M - |A_i \cup \{k\}|)^3}. \tag{A.31}$$

The corresponding noise power for conjugate beamforming, CIC, and CINC are simple extensions of the expressions from Equation A.29 to A.31. Conjugate beam-

forming is equivalent to CIN with $A_i = \emptyset$, so that

$$\mathbb{E}[|\text{noise}|^2_{cj}] = \frac{MN_0}{(M-1)[(M-1)^2-1]} \tag{A.32}$$

$$= \frac{MN_0}{(M-1)^3} + O\left(\frac{1}{(M-1)^5}\right) \tag{A.33}$$

$$\approx \frac{MN_0}{(M-1)^3}. \tag{A.34}$$

CIC has the same noise power as conjugate beamforming, yielding

$$\mathbb{E}[|\text{noise}|^2_{cj}] = \mathbb{E}[|\text{noise}|^2_{CIC}]. \tag{A.35}$$

In CINC, only amplify-and-forward signals that aren't part of the decode-and-forward set are used in the decorrelator, allowing us to replace A_i with $A_i \setminus D_i^k$ in Equations A.29 to A.31, yielding

$$\mathbb{E}[|\text{noise}|^2_{CINC}] = \frac{MN_0 + \frac{P_M(M+3)+K}{P_S K} N_{0,s}|A_i \setminus D_i^k \setminus \{k\}|}{(M - |A_i \setminus D_i^k \cup \{k\}|)[(M - |A_i \setminus D_i^k \cup \{k\}|)^2 - 1]} \tag{A.36}$$

$$= \frac{MN_0 + \frac{P_M(M+3)+K}{P_S K} N_{0,s}|A_i \setminus D_i^k \setminus \{k\}|}{(M - |A_i \setminus D_i^k \cup \{k\}|)^3} + O\left(\frac{1}{(M - |A_i \setminus D_i^k \cup \{k\}|)^5}\right) \tag{A.37}$$

$$\approx \frac{MN_0 + \frac{P_M(M+3)+K}{P_S K} N_{0,s}|A_i \setminus D_i^k \setminus \{k\}|}{(M - |A_i \setminus D_i^k \cup \{k\}|)^3}. \tag{A.38}$$

References

[1] C. Shepard, H. Yu, N. Anand, E. Li, T. Marzetta, R. Yang, and L. Zhong, "Argos: Practical many-antenna base stations," in *Proceedings of the 18th annual international conference on Mobile computing and networking*. ACM, 2012, pp. 53–64. 1

[2] T. L. Marzetta, "Noncooperative cellular wireless with unlimited numbers of base station antennas," *Wireless Communications, IEEE Transactions on*, vol. 9, no. 11, pp. 3590–3600, 2010. 1

[3] H. Yang and T. L. Marzetta, "Performance of conjugate and zero-forcing beamforming in large-scale antenna systems," *Selected Areas in Communications, IEEE Journal on*, vol. 31, no. 2, pp. 172–179, 2013. 1

[4] M. M. da Silva and F. A. Monteiro, *MIMO Processing for 4G and Beyond: Fundamentals and Evolution*. CRC Press, 2014. 1

[5] P. W. Wolniansky, G. J. Foschini, G. Golden, and R. A. Valenzuela, "V-blast: An architecture for realizing very high data rates over the rich-scattering wireless channel," in *Signals, Systems, and Electronics, 1998. ISSSE 98. 1998 URSI International Symposium on*. IEEE, 1998, pp. 295–300. 1

[6] J. Bai and A. Sabharwal, "Distributed full-duplex via wireless side-channels: Bounds and protocols," *Wireless Communications, IEEE Transactions on*, vol. 12, no. 8, pp. 4162–4173, 2013. 1

[7] O. Sahin and E. Erkip, "Achievable rates for the gaussian interference relay channel," in *IEEE GLOBECOM 2007-IEEE Global Telecommunications Conference*. IEEE, 2007, pp. 1627–1631. 1

[8] S. Sridharan, S. Vishwanath, S. A. Jafar, and S. Shamai, "On the capacity of cognitive relay assisted gaussian interference channel," in *2008 IEEE International Symposium on Information Theory*. IEEE, 2008, pp. 549–553. 1

[9] H. Kwon and J. M. Cioffi, "Multi-user MISO broadcast channel with user-cooperating decoder," in *Vehicular Technology Conference, 2008. VTC 2008-Fall. IEEE 68th.* IEEE, 2008, pp. 1–5. 1

[10] A. Kwong and A. Sabharwal, "Cooperative inter-beam nulling: A side-channel strategy for managing inter-beam interference," in *2015 49th Asilomar Conference on Signals, Systems and Computers.* IEEE, 2015, pp. 1242–1246. 3.1

[11] T. Kailath, H. Vikalo, and B. Hassibi, "MIMO receive algorithms," *Space-Time Wireless Systems: From Array Processing to MIMO Communications*, 2005. 3.1.2

[12] B. Collins, S. Matsumoto, and N. Saad, "Integration of invariant matrices and moments of inverses of ginibre and wishart matrices," *Journal of Multivariate Analysis*, vol. 126, pp. 1–13, 2014. A.2

[13] D. Maiwald and D. Kraus, "Calculation of moments of complex wishart and complex inverse wishart distributed matrices," in *Radar, Sonar and Navigation, IEE Proceedings-*, vol. 147, no. 4. IET, 2000, pp. 162–168. A.3, A.3